Petroleum Science (2019) 16:591–605
https://doi.org/10.1007/s12182-019-0304-z

ORIGINAL PAPER

How much would silica nanoparticles enhance the performance of low-salinity water flooding?

Amir Hossein Saeedi Dehaghani[1] · Reza Daneshfar[2]

Received: 5 March 2018 / Published online: 18 March 2019

Abstract
Nanofluids and low-salinity water (LSW) flooding are two novel techniques for enhanced oil recovery. Despite some efforts on investigating benefits of each method, the pros and cons of their combined application need to be evaluated. This work sheds light on performance of LSW augmented with nanoparticles through examining wettability alteration and the amount of incremental oil recovery during the displacement process. To this end, nanofluids were prepared by dispersing silica nanoparticles (0.1 wt%, 0.25 wt%, 0.5 wt% and 0.75 wt%) in 2, 10, 20 and 100 times diluted samples of Persian Gulf seawater. Contact angle measurements revealed a crucial role of temperature, where no wettability alteration occurred up to 80 °C. Also, an optimum wettability state (with contact angle 22°) was detected with a 20 times diluted sample of seawater augmented with 0.25 wt% silica nanoparticles. Also, extreme dilution (herein 100 times) will be of no significance. Throughout micromodel flooding, it was found that in an oil-wet condition, a combination of silica nanoparticles dispersed in 20 times diluted brine had the highest displacement efficiency compared to silica nanofluids prepared with deionized water. Finally, by comparing oil recoveries in both water- and oil-wet micromodels, it was concluded that nanoparticles could enhance applicability of LSW via strengthening wettability alteration toward a favorable state and improving the sweep efficiency.

Keywords Low-salinity water · Silica nanoparticles · Low-salinity nanofluid · Micromodel · Enhanced oil recovery · Wettability alteration

1 Introduction

Despite advances with different enhanced oil recovery (EOR) methods, it is well understood that a great amount of petroleum remains unrecovered in underground reservoirs (Bera and Belhaj 2016). With the advent of nanoscience and emergence of its potential, researchers have investigated the applicability of nanoparticles in the upstream petroleum industry (Barati-Harooni et al. 2016; Emadi et al. 2017; Rezaei et al. 2016). Recent studies have pointed out advantages of utilizing nanofluids as EOR agents, which have not been considered enough (Fletcher and Davis 2010; Rezvani et al. 2017). Generally, the underlying mechanisms of improving oil recovery by injecting nanoparticles fall into six categories, including: (1) establishing disjoining pressure to aid detachment of oil drops from the pore surface (Chengara et al. 2004; Mcelfresh et al. 2012; Wasan et al. 2011), (2) plugging pore channels (Hashemi et al. 2013; Idogun et al. 2016; Sun et al. 2017; Zamani et al. 2012), (3) enhancing sweep efficiency by decreasing the mobility of the displacing fluid (Al-Anssari et al. 2016; Salem Ragab and Hannora 2015; Tarek and El-Banbi 2015), (4) altering rock wettability toward water-wet conditions (Hendraningrat and Torsæter 2014a; Hendraningrat and Torsaeter 2014b; Karimi et al. 2012; Li et al. 2015; Mohebbifar et al. 2015), (5) reducing interfacial tension (IFT) between residual oil and injecting fluids (Alomair et al. 2014; Hendraningrat et al. 2013a; Salem Ragab and Hannora 2015; Torsater et al. 2012) and (6) preventing/retarding asphaltene precipitation by the action of nanoparticles (Haindade et al. 2012; Kazemzadeh et al. 2015; Nassar et al. 2012; Tarboush and Husein 2012).

Edited by Yan-Hua Sun

✉ Amir Hossein Saeedi Dehaghani
asaeedi@modares.ac.ir

[1] Department of Petroleum Engineering, Faculty of Chemical Engineering, Tarbiat Modares University, Jalal Ale Ahmad Highway, Gisha Bridge, Tehran, Iran

[2] Department of Petroleum Engineering, Ahwaz Faculty of Petroleum Engineering, Petroleum University of Technology (PUT), Ahwaz, Iran

Among various EOR methods, low-salinity water (LSW) flooding has greatly attracted the notice of petroleum researchers partly due to availability of vast natural water resources and also being an environmental-friendly approach (Sheng 2014). Numerous experimental studies have indicated unexpected capabilities of LSW for improving oil recovery in comparison with conventional flooding of untreated, high-salinity formation water (FW) (Aghaeifar et al. 2015; Morrow and Buckley 2011; Morrow et al. 1998; Rivet et al. 2010; Tang and Morrow 1997, 1999b, c, 2002). Currently, researchers have unanimously regarded wettability alteration as the main reason for applying LSW to bring about additional oil recovery (Jalili and Tabrizy 2014; Kafili Kasmaei and Rao 2015; Mahani et al. 2015; Shabib-Asl et al. 2014; Shaddel et al. 2014; Yang et al. 2015). In this respect, various mechanisms have been proposed to explain the low-salinity effect (LSE) as follows: (1) osmotic pressure (Buckley and Morrow 2010), (2) IFT reduction in response to an increase in reservoir fluid pH (McGuire et al. 2005), (3) multicomponent ion exchange (MIE) (Lager et al. 2008), (4) double-layer expansion (Ligthelm et al. 2009), (5) dissolution of heavy oil components by the salting in effect (Rezaei-Doust et al. 2009), (6) saponification (McGuire et al. 2005) and (7) elasticity of water films lying on pore walls (Buckley and Morrow 2010). While wettability alternation is considered as the main mechanism behind LSE, the understanding of which factors control the wettability variation is incomplete due to the complexity of the interactions occurring in the oil/brine/rock system. The two approaches that reveal the controlling factors behind the wettability alteration are (a) double-layer expansion between fine particles and limited fines release (LFR) between oil/rock contact areas (Nasralla and Nasr-El-Din 2014; Tang and Morrow 1999a; Xie et al. 2016) and (b) surface complexation modeling (Brady and Krumhansl 2012; Brady and Thyne 2016; Brady et al. 2015; Mahani et al. 2017; Xie et al. 2017).

To evaluate the potential of nanoparticles as novel EOR agents, some studies have been performed on silica (SiO_2) nanoparticles dispersed in deionized water using a glass micromodel as a synthetic porous media (El-Diasty 2015; Gharibshahi et al. 2015; Heydarian et al. 2012; Li et al. 2016; Maghzi et al. 2012; Mohammadi et al. 2012; Ragab and Hannora 2015; Salem Ragab and Hannora 2015). Likewise, many others have investigated LSE in the micromodel (Bondino et al. 2013; Emadi and Sohrabi 2012, 2013; Fredriksen et al. 2016; Maaref et al. 2017; Song and Kovscek 2015; Wei et al. 2017). In light of those studies, one could conceive the question of how much would the benefit be of utilizing LSW augmented by nanoparticles? Naturally, exploiting simultaneous advantages of nanotechnology and LSW may bring about a higher improvement in oil recovery. To the best of our knowledge, few studies have investigated the effect of silica nanoparticles dispersed in brine for oil displacement in porous media. Among them, Torsater et al. (2012) observed an 8% incremental oil recovery by injecting SiO_2 nanofluids after water flooding into an oil-saturated sandstone core. In another work, Parvazdavani et al. (2012) made an effort to probe the relative permeability of displacing/displaced fluids by means of injecting plain water or a 1 wt% SiO_2 nanofluid prepared with brine into an oil-saturated sandstone core. They obtained relative permeability curves for flowing phases (oil and nanofluid) and pointed out higher oil relative permeability while using silica nanoparticles. Also, by measuring interfacial tension (IFT) of water/oil and oil/nanofluid systems, they ascribed higher oil relative permeability to the IFT reduction which took place during nanofluid injection.

Li et al. used 3 wt% brine thickened by SiO_2 nanoparticles (0.01 wt%, 0.05 wt% and 0.1 wt%) for displacing residual oil in a micromodel and a sandstone core. They observed that using nanoparticles had reduced the IFT while contacting the oil phase and shifted the wettability of porous media surfaces toward water wetness. Moreover, they obtained an ~ 5% incremental oil recovery by displacing in situ oil by the nanofluid in comparison with secondary mode water flooding (Li et al. 2013). In a later study, they utilized more concentrated fluids (0.05 wt%, 0.1 wt% and 0.5 wt% SiO_2 nanoparticle) and again observed a tendency of the oil-wet micromodel surface to shift toward water wetness once it contacted the silica nanofluid. In this fashion, there was a direct proportionality between the degree of wettability alteration and the concentration of nanoparticles (Li and Torsæter 2014). In a further step, Li et al. (2015) scrutinized the degree of wettability alteration by performing imbibition tests on sandstone plugs with brine (3 wt% NaCl) containing dispersed SiO_2 nanoparticles, and pointed out a strong tendency of nanofluid to be imbibed into the oil-saturated plug.

To evaluate the capability of nanofluids for mobilizing oil trapped in tortuous pores, Aurand et al. (2014) carried out core flood experiments by injecting North Sea brine having 0.05 wt% SiO_2 nanoparticles and observed 20% incremental recovery after flushing the core plug with plain water. Analogously, Alomair et al. observed the effect of SiO_2 nanoparticles on the incremental oil recovered through tertiary mode injection, i.e., when water flooding cannot sweep residual oil. In this way, they observed a maximum recovery (~ 6%) at 0.01 wt% of nanoparticles. However, severe pore plugging occurred as a result of nanofluid instability and subsequent deposition at higher SiO_2 concentrations (Alomair et al. 2014). In a similar study, Hendraningrat et al. (2013b) proceeded with using silica nanofluids for flooding oil-saturated sandstone cores and demonstrated the importance of the nanoparticle concentration, where the maximum incremental oil recovery (25%) occurred at 0.05 wt% nanofluid. Later, they investigated the effect of nanoparticle diameter (7, 16 and 40 nm) and pointed out that the highest oil recovery was achieved using the smallest nanoparticles (Hendraningrat et al. 2013c).

Based on the aforementioned studies, silica nanoparticles form an effective agent to be employed for EOR. However, it should be emphasized that most of the previous works have only used sodium chloride (NaCl) for brine preparation and the impact of other ions has been neglected (Hendraningrat et al. 2013b; Li et al. 2013; Li and Torsæter 2014; Torsater et al. 2012) and most of them used high-salinity brine to disperse nanoparticles (Aurand et al. 2014; Hendraningrat et al. 2013b, c; Li and Torsæter 2014; Li et al. 2013). Also, only Li and co-workers carried out a thorough investigation on SiO_2 nanofluids using a micromodel as the porous substrate (Li et al. 2013; Li and Torsæter 2014). Therefore, there is a lack of understanding of the extend of oil recovery using SiO_2 as an additive to LSW.

In this study, performance of silica nanoparticles dispersed in low-salinity water was investigated in terms of wettability modification, quantified by contact angle measurements and displacement efficiency with injection into a glass micromodel. For this purpose, we used diluted samples of synthetic Persian Gulf seawater for injection. The core of our experiments includes: examining the stability of SiO_2 in LSW, contact angle measurements at varying concentrations and temperatures, and finally, evaluating oil displacement efficiency of low-salinity nanofluids by injecting them into glass micromodels.

2 Experimental

2.1 Materials

The oil used in this study with a specific gravity of 33°API was taken from a field in southwest Iran. Silica nanoparticles with 98% purity, 20 nm in diameter and a specific surface area of 20 m^2/g were purchased from Merck (Germany). Ultra-deionized water of conductivity 0.2 µS/cm was used to prepare nanofluids containing varying concentrations of salts and nanoparticles. In this research, the base brine (synthetic Persian Gulf seawater) was prepared by dissolving different salts (NaCl, KCl, $CaCl_2$, Na_2SO_4, $MgCl_2 \cdot 6H_2O$ and $NaHCO_3$). They were all purchased from Merck. Hexamethyldisilane, $Si_2(CH_3)_6$, was used for turning the original wettability of the micromodels from strongly water wet to oil wet. Also, methanol (CH_3OH) and toluene (C_7H_8), both of 99% purity, were used as washing and wettability-altering agents, respectively. In this research, the seawater (SW) was synthesized with the same composition as the Persian Gulf seawater. The salts used and ions and their concentrations are presented in Table 1. Also, the physical properties of the crude oil are listed in Table 2.

2.2 Apparatus

2.2.1 Sessile drop

The most popular method for determining contact angles with sessile drops is the goniometric technique that was used in this work. The images which were taken by a camera (3CCD Color Sony DXC-C33P Video Camera PAL) were analyzed by image processing software, to record contact angles accurately. A schematic of contact angle measurement using the sessile drop method is depicted in Fig. 1.

2.2.2 Micromodel

For visual inspection of oil displacement processes, a microfluidic device (micromodel) was utilized, which is a two-dimensional glass sheet with narrow conduits (pores) etched on its surface. This transparent device represents the pore structure of sandstone. It consists of a 6×6 cm^2 matrix and etch depth of 6 µm, corresponding to a porous media having 38% porosity and 0.22 cm^3 pore volume (PV). With the aid of a photolithography technique, first the underlying pattern of the porous medium was etched on a silicon wafer to achieve a homogenous pattern with coordination number of 4, which means every pore body is connected to 4 neighboring pores on average. This standard pattern has typically been employed in previous work (Wu et al. 2016a, b; Wang et al. 2014; Kazempour et al. 2014). It was polished to obtain a smooth pattern by removing any unwanted residues. Afterward, two holes were drilled at two opposite corners of the glass plane to provide input and output conduits of the porous medium for fluid injection and production, respectively, as depicted in Fig. 2. Contrary to most conventional micromodels, our model permits investigating sweeping performance by imitating a five-spot injection pattern adopted in most classical EOR studies (Sheng

Table 2 Crude oil characterization

Asphaltene content, wt%	Density, g/cm^3	Viscosity at 10 °C, cP
9.51	0.86	30

Table 1 Composition of the synthetic Persian Gulf seawater

Ion concentration, mol/L							TDS, mg/L
Na^+	K^+	Ca^{2+}	Mg^{2+}	Cl^-	HCO_3^-	SO_4^{2-}	
0.13	0.649	0.536	0.012	0.758864	0.033	0.012	41369

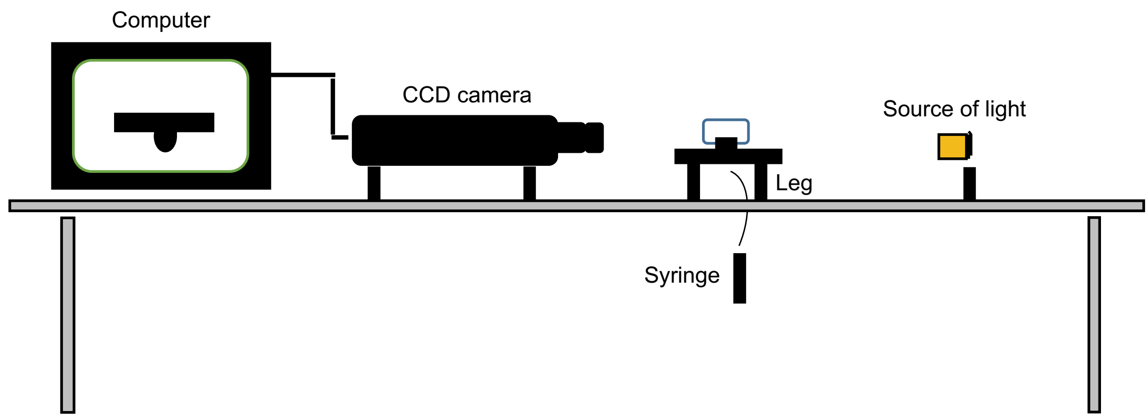

Fig. 1 Sessile drop apparatus for measuring contact angles

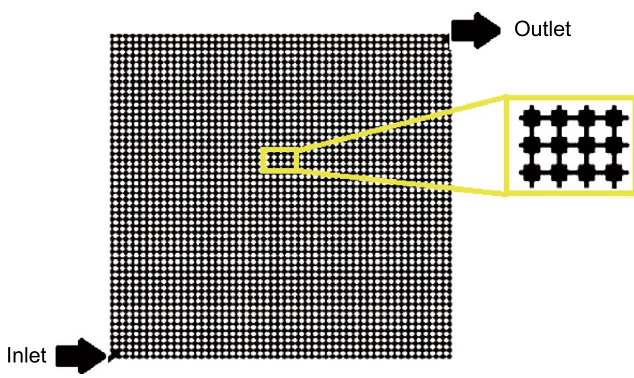

Fig. 2 A schematic of the pore network structure of the micromodel. Inset shows a magnified image of etched pores

2010; Green and Willhite 1998). This structure was chosen to allow observation of the fluid front to obtain insight into the effect of viscosity on the displacement process.

Once the etched glass was prepared, it was bonded to a flat piece of glass and put in a furnace and fused at 700 °C. At high temperature, the glass plates stick to each other to make a unified piece, having only the etched pattern and the drilled holes open for flow. Also, exposing the glass surface to oxygen at a high temperature generates a layer of silica (SiO_2), which constitutes the main part of natural sandstones. With this, one could obtain a strongly water-wet substrate similar to intact underground quartz minerals. Table 3 summarizes the main characteristics of the micromodel used in this work.

3 Experimental

3.1 Design of experiments

In this research, contact angle measurements were conducted for different salinity fluids with varying ionic strengths and nanoparticle concentrations.

The different salinity nanofluids were prepared with 2, 5, 10, 20 and 100 times diluted seawater (named 2-TDSW, 5-TDSW, 10-TDSW, 20-TDSW and 100-TDSW). To account for both parameters simultaneously and reducing the number of trials, nanofluids were prepared according to the values specified in Table 4. SW was diluted up to 100 times of the original composition [the extreme case of dilution reported in previous work (Fjelde et al. 2012)] with a maximum of 1 wt% dispersed SiO_2 nanoparticles (the extreme case of SiO_2 nanoparticle concentration reported in most previous works).

Table 3 Characteristics of the glass micromodel used as a porous medium

Texture	Injection pattern	Porosity, %	Dimensions, cm × cm × cm	Pore volume, cm^3
Homogenous	1/4 Five spot	38	6 × 6 × 0.006	0.22

Table 4 Fluids prepared with synthetic seawater

Extent of dilution	1	2	5	10	20	100
Nanoparticle concentration, wt%	0	0.10	0.25	0.50	0.75	1.00

3.2 Preparation of nanofluid

Two fluids, with and without nanoparticles, were used in contact angle and injection experiments. The nanofluids were prepared by adding nanoparticles to brines with different salinity, which were obtained from dilution of SW, and then homogenized by a magnetic stirrer at 400 rpm for 30 min. In the next step, the nanofluids were sonicated using an ELMA Elmasonic 1.5-Gal Tabletop Ultrasonic Cleaner, P60H, for 30 min to ensure complete dispersion of nanoparticles.

3.3 Preparation of the oil-wet micromodel

The following steps were taken to alter the wettability of the micromodel toward oil wetness:

(a) The micromodel was rinsed with a sodium hydroxide (NaOH) solution and soaked in it for 1 h.
(b) The micromodel was then rinsed with deionized water and dried in an oven for at least 15 min at 200 °C to ensure no residue remained on its surface.
(c) The micromodel was soaked in a solution of 2% hexamethyldisilane and 98% anhydrous toluene for 5 min. At the end, a thin hydrophobic layer repelling water droplets was observed covering the glass surface.
(d) Lastly, the micromodel was rinsed with methanol in order to purge any excess silicon fluid and then was dried in an oven at 100 °C to strengthen the adsorbed silicon layer.

3.4 Contact angle measurement

At first, square glass slabs (1.5×1.5 cm^2) were cut and submerged in toluene to remove any undesirable adsorbed oleic components. Afterward, the contact angle of a water drop was measured on the glass surfaces to ensure they were initially in a strongly water-wet state. The slab wettability was then changed to an oil-wet state following the procedure detailed below. Once oil-wet slabs were obtained, they were immersed in the nanofluid, comprised of diluted brine and nanoparticles, in an attempt to restore their original water wetness. This latter process was repeated at varying concentrations of nanoparticles and brine salinity to evaluate wettability by contact angle measurement. For this purpose, the sessile drop method was applied, where a drop of *n*-heptane (representing the oleic phase) was injected into a cell, full of deionized water, at constant temperature (25 °C). Naturally, the drop moves upward driven by buoyancy force and touches the glass slab, as shown in Fig. 1. A high-resolution camera and a microscope captured pictures of the drop on the glass slab in three modes, namely initial, original oil-wet and modified wettability states. The error of measured contact angles is ± 5°, and error bars are shown in the following figures. In this work, each contact angle was measured three times and the average has been reported.

3.5 Micromodel flooding

Before proceeding to this stage, the stability of nanofluids was confirmed at different nanoparticle concentrations to avoid any unwanted precipitation or pore plugging by nanoparticle deposition. To this end, all fluids were checked visually to be sufficiently transparent.

Flooding processes were conducted under ambient conditions (25 °C and 1 atm), and the micromodel was mounted horizontally to exclude any effect of gravity. Figure 3 shows the schematic of the flooding setup consisting of the micromodel (detailed earlier), a syringe pump (Harvard Apparatus, Holliston, MA) and a high-resolution camera (Canon VIXIA HF S200 HD Camcorder). The flooding procedure could be summarized as follows:

(a) Initially, the pores of the micromodel were preflushed with toluene to ensure that no oil was left in the micromodel.
(b) The micromodel was evacuated to remove any possible trapped solvents, fluids or air.
(c) To achieve a fully oil-saturated model, the syringe pump injected oil into the pores at a rate of 0.05 mL/h.
(d) After saturating the micromodel, the nanofluid was injected at a rate of 0.05 mL/h to push the oil out of the model. This was performed using the syringe pump. At the same time, a camera placed above the micromodel took images at 2-minute intervals to monitor fluid front advancement in the porous media and also to allow a later oil recovery calculation.
(e) Eventually, the images were analyzed by image processing software, to obtain the amount of oil recovery by counting pixels of the image representing oil spots in the model.

3.6 Turning micromodel wettability to oil wetness

The micromodel was placed in a 1:1 methanol/toluene volumetric mixture to ensure having an entirely clean surface, without any attached organic impurities. To verify the water-wet state of the glass surfaces, the contact angle of an *n*-heptane drop in deionized water was measured on those surfaces, as shown in Fig. 4.

Once clean glass surfaces were prepared, they were immersed in an oleic mixture (2% hexamethyldisilane and 98% toluene) for 30 min, to make them oil-wet surfaces. Subsequently, they were dried for 2 h in an oven at 80 °C. Afterward, those surfaces were drenched in synthetic formation water with a salinity of 180,000 ppm

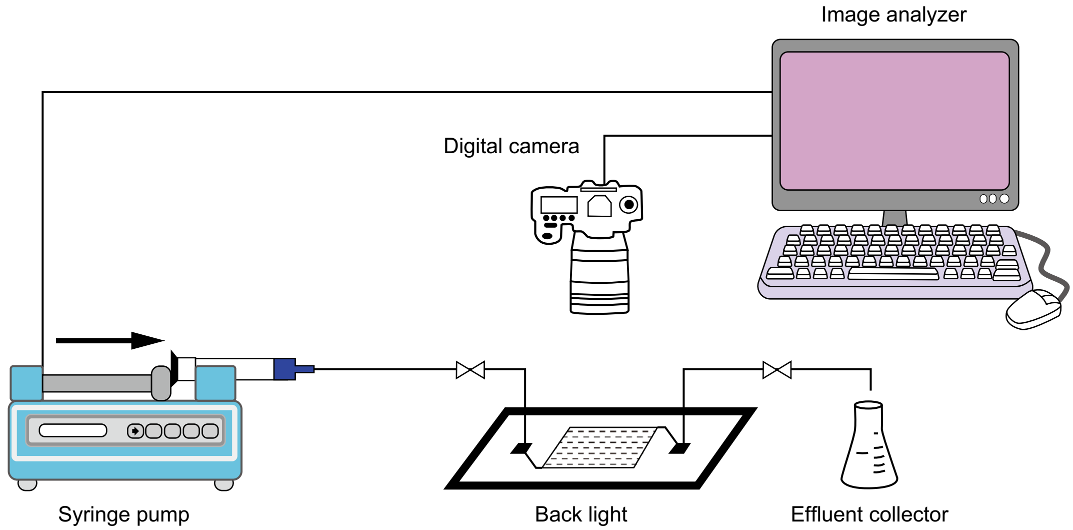

Fig. 3 Schematic of the flooding setup

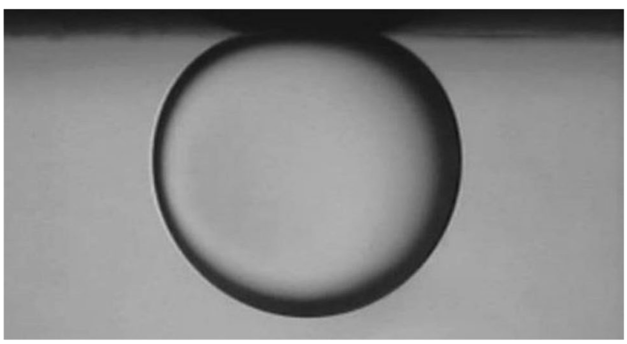

Fig. 4 *n*-Heptane droplet contacting the water-wet glass surface

Fig. 5 *n*-Heptane droplet contacting the oil-wet glass surface

NaCl and then were placed in crude oil for 12 h at 80 °C. Once again, samples were rinsed with toluene and dried at 80 °C. Eventually, the oil-wet tendency of the treated surfaces was probed by measuring the contact angle by a heptane droplet in deionized water. Through this soaking/drying procedure, one could obtain oil-wet slabs representing wetting characteristics of real reservoir conditions. Although using hexamethyldisilane is a common practice for making glass surfaces oil wet, we also made use of crude oil to heighten accuracy of the treatment and as shown in Fig. 5, the glass surfaces became completely oil wet. This procedure was done by aging oil-wet slabs in crude oil at ambient conditions (25 °C and 1 atm) for 48 h; and then the slabs were washed with toluene to remove extra oil from them to prepare for contact angle measuring tests. The contact angles for all slabs were measured after the aging time showing a complete oil-wet condition (~ 180°).

4 Results and discussion

In this section, we discuss the results of oil–water contact angle measurements, stability of nanofluids and oil recovery during injection of the nanofluids at varying salinities.

4.1 Nanofluid stability

Turbidity is a measure of assessing stability of suspensions over time. In this method, the reflection of a light beam shone through fluid records its stability and is recorded in nephelometric turbidity units (NTU). The stability curve of 20-TDSW containing varying concentrations of nanoparticles is shown in Fig. 6. The sample stability is related to nanoparticle concentrations, where diluted ones show constant NTU versus time. Noteworthy, all samples showed good stability in the first 72 h, ensuring that wettability and flooding experiments have been performed with stable fluids. Based on similar measurements, the turbidity of the samples of silica nanoparticles dispersed in deionized water (salinity 0) with different concentrations (0.10, 0.25, 0.50, 0.75, 1.00 and 2.00 wt%) remained approximately constant after 200 h. The results are presented in Table 5.

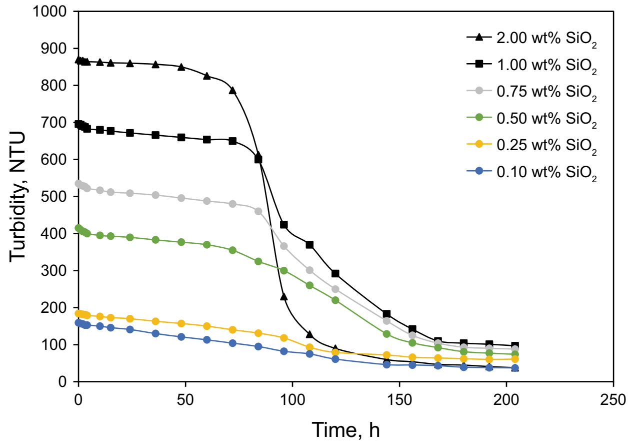

Fig. 6 Turbidity of low-salinity nanofluids at varying concentrations of nanoparticles dispersed in 20-TDSW

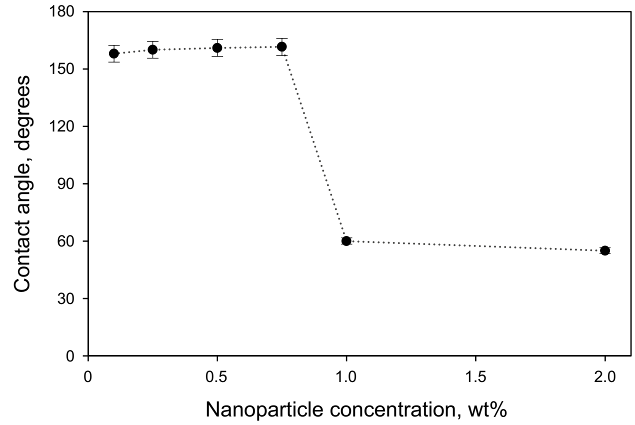

Fig. 7 Effect of nanoparticle concentrations on the contact angle of *n*-heptane droplet on the glass surface (nanofluids prepared with deionized water)

Table 5 Turbidity (in NTU) of the samples of silica nanoparticles dispersed in deionized water at different concentrations

Nanoparticle concentration, wt%	Time, h	
	0	200
0.10	143	143
0.25	164	163
0.50	395	395
0.75	509	508
1.00	606	605
2.00	816	815

4.2 The effect of nanoparticle concentration in deionized water (salinity 0) on wettability of treated glass surfaces

The effect of nanofluids on the wettability of treated (oil-wet) glass surfaces was investigated at varying nanoparticle concentrations after 3 days of soaking at the ambient temperature (25 °C). In this section, the nanofluids used were prepared by dispersing nanoparticles in deionized water, i.e., the salinity of these nanofluids was zero. As shown in Fig. 7, the contact angle was nearly constant (~ 160°) up to 0.75 wt% nanoparticle concentration. However, a dramatic reduction occurred at higher nanoparticle concentrations, reflecting an abrupt change in the glass surface wettability toward water wetness. Increasing the concentration of silica nanoparticles above a threshold value, somewhere between 0.75 wt% and 1.00 wt%, brought about a large shift of the oil-wet glass surface to a practically water-wet state, with a contact angle of ~ 60°. On the other hand, the wettability remains almost constant with a further increase in the nanoparticle concentration in the soaking fluid, up to 2.00 wt%, as shown in Fig. 7. The interesting steplike diagram of Fig. 7 suggests that nanofluids used in this study would be effective once the nanoparticle concentrations were greater than a critical value, that is, 0.75 wt% in the conditions prevailing for this study. Besides undesirable instability of the solution, as shown in Fig. 6, using highly concentrated nanofluid has no appreciable influence on altering wettability toward the favorable state, which imposes a major economical constriction on their applicability.

At this point, one question arises. What is the mechanism underlying this peculiar observation? Previous studies have confirmed that coating glass or rock surfaces with nanoparticles alter their wettability. However, based on our observation, one cannot attribute wettability alteration solely to adsorption of nanoparticles on glass surfaces. The structural disjoining pressure is the plausible mechanism behind the observed phenomenon. In this mechanism, negatively charged nanoparticles diffuse around oil droplets lodged on the glass surface. Recalling that the water–oil interface beneath the oil droplet is of negative charge, except at the high pH and ionic strength relevant to the formation brines (Jackson et al. 2016) and/or in highly acidic crude oil (Buckley 1999), as a result, repulsion between the interfaces leads to detachment of oil droplets from the surface by nanoparticles, and consequently, wettability changes the glass surface from oil wet toward water wet.

To provide an insight into effect of the soaking period on wettability alteration, the experiment was conducted again in 6 days. As shown in Fig. 8, there is no difference between the trend of the earlier test and the latter, except for a further reduction in contact angle at 1.00 wt% and 2.00 wt% nanoparticle concentrations as a result of longer soaking time of glass surface in the nanofluids.

4.3 Effect of seawater dilution on wettability of treated glass surfaces

In this research, synthetic Persian Gulf brine (called SW) was used as the base fluid to investigate the effect of brine

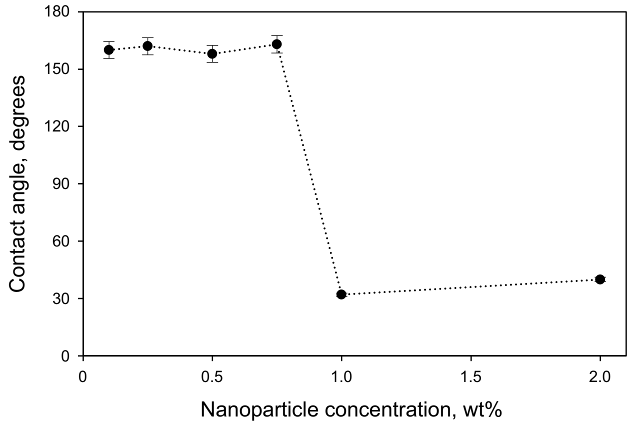

Fig. 8 Effect of nanoparticle concentrations on the contact angle of *n*-heptane droplet on the glass surface after 6 days

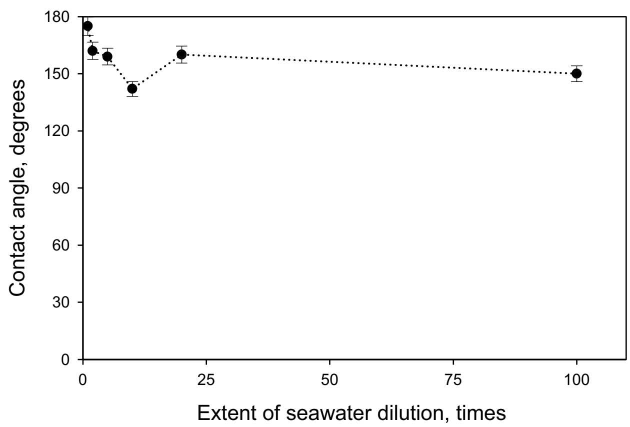

Fig. 9 Effect of seawater dilution on wettability alteration of the oil-wet treated glass surface at 25 °C

dilution extent on wettability alteration. For this purpose, SW was diluted 2, 5, 10, 20 and 100 times (in short 2-TDSW, 5-TDSW, 10-TDSW, 20-TDSW and 100-TDSW) by mixing with deionized water. Treated oil-wet glass surfaces were submerged in each brine sample for 3 days at environmental temperature (25 °C). It was observed that brine dilution has a negligible effect on wettability of the glass surface, as demonstrated in Fig. 9. In contrast, repeating the experiment at 80 °C revealed a marked influence of dilution on changing the wetting, as shown in Fig. 10. Unsurprisingly, as well understood in previous work (Al-Aulaqi et al. 2011a, b), ions are more active at higher temperatures and could contribute to interfaces more effectively, as pointed out by Agbalaka et al. (Agbalaka et al. 2009). By measuring the Amott–Harvey wetting index for sandstone cores, they understood that a temperature increment of low-salinity brines would make the core samples more water wet. Noteworthily, dilution above 10 times has reduced the contact angle of oil-wet glass surface by ~ 80°. Additionally, once the abrupt change took

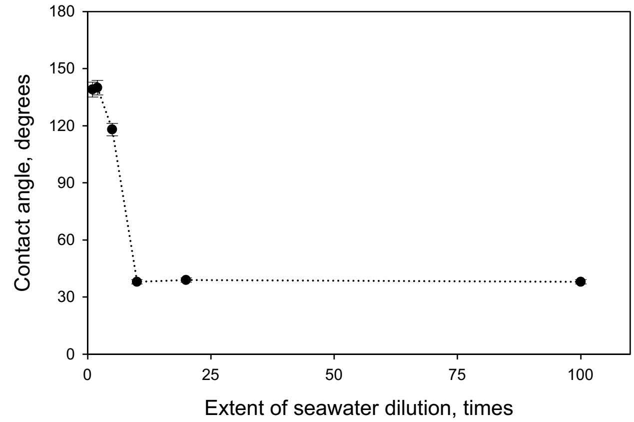

Fig. 10 Effect of seawater dilution on wettability alteration of the oil-wet treated glass surface at 80 °C

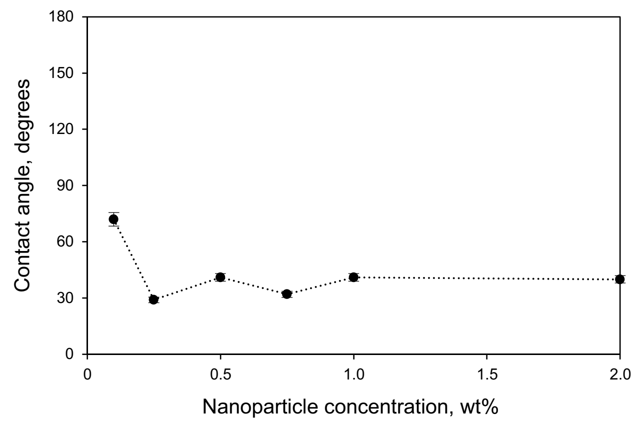

Fig. 11 Contact angle of *n*-heptane droplet on the treated (oil-wet) glass surface at varying concentrations of nanoparticles dispersed in 20-TDSW

place, further dilution of the SW (20 and 100 times) did not reduce the contact angle any further. This behavior is analogous to that observed for the variation in nanoparticle concentrations, as shown in Fig. 8.

4.4 Simultaneous influence of nanoparticles and seawater salinity on wettability of treated glass surfaces

Based on the preceding experiments, the 20 times diluted seawater (20-TDSW) was chosen as the base fluid and was thickened by varying concentrations of nanoparticles. As shown in Fig. 11, the nanofluid could incredibly restore the original (untreated) water wetness of the glass surfaces, as a result of the synergic effect of silica nanoparticles and seawater salinity. This observation points to the beneficial aspect of applying nanotechnology in conjunction with low-salinity water flooding, which both are current research topics in petroleum engineering. The improved performance of the nanofluid for altering wettability in low-salinity environment supports our hypothesis that surface adsorption is not the sole cause of wettability alteration. The structural disjoining pressure, which was enforced simultaneously by the effect of nanoparticles as well as seawater salinity, leads to a contact angle reduction, as shown in Fig. 11. However, this trend is somewhat erratic, suggesting that there is no point in using high concentrations of SiO_2 nanofluid more than 0.25 wt%, which was discussed in the preceding section.

In another attempt, the effect of salinity on glass wettability was investigated with different salinity nanofluids containing 0.25 wt% SiO_2 nanoparticles. These nanofluids were prepared by dispersed SiO_2 nanoparticles in synthetic SW, 2-TDSW, 5-TDSW, 10-TDSW, 20-TDSW and 100-TDSW, and the contact angle of *n*-heptane was measured on the treated (oil-wet) glass surface. As shown in Fig. 12, 0.25 wt% nanofluid prepared with 2-TDSW results in a sharp reduction in contact angle, that is, restoring the original (untreated) wettability state of the glass surface. Nevertheless, further dilution was of mild influence on wettability alteration in achieving the minimum contact angle of 22° at 20-TDSW. It was notable that at an extreme dilution level, dissolved ions would be of minimal activity, where the diluted brine would act like deionized water. In support of this argument, no wettability alteration effect was observed in the case of 100-TDSW, as shown in Fig. 12.

4.5 Oil recovery

After analyzing the effect of dilution (i.e., brine salinity) and nanoparticle concentration on the wettability of the glass surface, here we proceed to a higher-scale micromodel network, to evaluate the contribution of wettability alteration to oil displacement by nanofluid injection. It has been well understood that the distribution of oil and water phases in a porous media is proportional to the wettability of its pore structure. Intuitively, one would expect a direct relation between the oil displacement efficiency and the degree of wettability alteration by the injected fluid, herein low-salinity SiO_2 nanofluid.

By injecting 0.25 wt% SiO_2 nanofluid prepared with 20-TDSW or 1.00 wt% nanofluid prepared with deionized water into the oil-saturated micromodel, we observed oil recovery enhancement while using suspensions with higher concentration. As shown in Fig. 13, the nanofluid containing 1.00 wt% SiO_2 particles resulted in higher oil recovery, 15% higher than the nanofluid containing 0.25 wt% SiO_2. Recall that the micromodel in this experiment was initially water wet, and as discussed earlier, no further wettability alteration would have occurred in the presence of nanoparticles, since the substrate was initially strongly water wet. As a result, some other mechanism(s) come(s) in effect to bring about a higher recovery while injecting a nanofluid with higher concentration. Among diverse properties associated with fluid displacement in porous media, viscosity is of paramount importance, as it affects both the rate and amount of ultimate oil recovery. To exclude any experimental artifact in this study, higher injection rates were used during injection scenarios to overcome capillary end effects (Al Harrasi et al. 2012; Hosseinzade Khanamiri et al. 2016), as discussed in the experimental section. As evident in Fig. 13, one could notice a delayed breakthrough in the case of injecting the 1.00 wt% SiO_2 nanofluid prepared with deionized water (with a salinity of 0) in comparison with the 0.25 wt% nanofluid with salinity of 0. Similar behavior was also observed in the case of 0.25 wt% SiO_2 nanofluid prepared with 20-TDSW. Increasing viscosity leads to lower

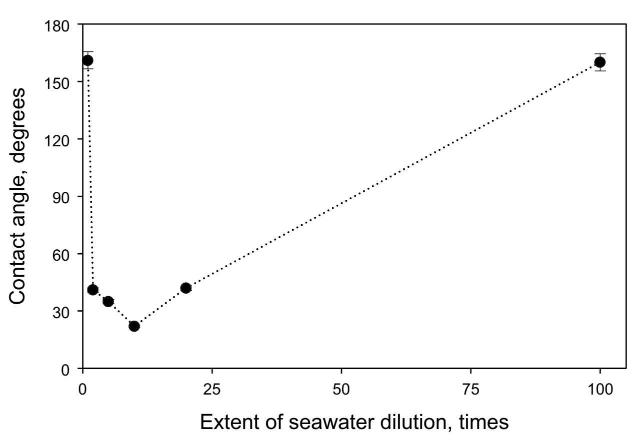

Fig. 12 Effect of salinity of nanofluids (0.25 wt%) on wettability of the oil-wet treated glass surface

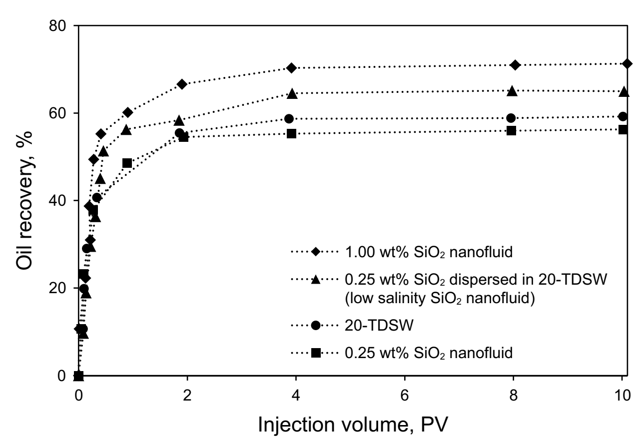

Fig. 13 Oil recovery during injection of different fluids into the water-wet micromodels. In this section, 1.00 wt% and 0.25 wt% SiO_2 nanofluids were prepared with deionized water, with a salinity of zero; 0.25 wt% of low-salinity SiO_2 nanofluid was prepared with 20-TDSW

mobility contrasts of the displacing (nanofluid) to displaced (oil) phases, and consequently, uniform displacement in pore networks is provided. Additionally, as inferred by the Buckley–Leveret theory (Buckley and Leverett 1942), decreasing mobility of the displacing fluid delays the breakthrough time, as exemplified in Fig. 13. Apart from the change of rheological characteristics, Brownian motion of silica nanoparticles induces their interaction with surface-active compounds at the oil–water interface by attracting natural surfactants on the interface, thus reducing the interfacial tension and as a result, higher oil recovery.

In a further evaluation, we repeated the foregoing experiment for the case of treated (oil-wet) micromodels. Contrary to the previous water-wet medium, we observed a maximum oil recovery of 62% when injecting 0.25 wt% of low-salinity SiO_2 nanofluid (prepared with 20-TDSW). As discussed earlier, brine dilution and the presence of nanoparticles both modified the wettability of glass substrate toward the favorable water-wet state. Maximum recovery as well as the longest breakthrough time was observed in the case of injecting 0.25 wt% of low-salinity SiO_2 nanofluid, which reflects a synergic contribution of wettability alteration and mobility reduction by increased viscosity. Interestingly, in contrast to results of the water-wet medium shown in Fig. 13, brine dilution and nanoparticle thickening have comparable influences on the ultimate oil recovery, as illustrated in Fig. 14. This figure also supports the advantage of utilizing nanoparticles in EOR processes, where 8% incremental recovery was achieved by blending 0.25 wt% nanoparticles in 20-TDSW. Figure 15 shows micromodel images used for sweep efficiency calculation. The images show the injection of the above fluids (0.25 wt% SiO_2 low-salinity fluid, 1.00 wt% SiO_2 nanofluid, 20-TDSW and formation water) into the treated (oil-wet) micromodel. From these images, it can be concluded that injection of 0.25 wt% of low-salinity SiO_2 nanofluid into the micromodel has the highest areal sweep efficiency. The images also indicate that formation water injection yields the lowest oil recovery among these injection scenarios.

Figure 16a compares oil recovery by injecting 0.25 wt% of low-salinity SiO_2 nanofluid into oil-wet and water-wet micromodels. There was a difference of 4% in oil recovery due to wettability alternation of pore networks. Although the low-salinity nanofluid is able to change the wetting state to a favorable one, oil-wet (treated) medium will not completely resume its original strongly water-wet characteristics during the short period of the displacement process. On the other hand, wettability restoration is a result of the synergic contribution of both low-salinity and dispersed nanoparticles. Figure 16b compares oil recovery via injecting 20-TDSW into oil-wet and water-wet micromodels, and there was a difference of 3% in oil recovery due to wettability alternation. In this respect, about 16% more recovery would be achieved by adding 0.25 wt% of SiO_2 nanoparticles to 20-TDSW in the case of the water-wet medium, by the comparison of Fig. 16a, b.

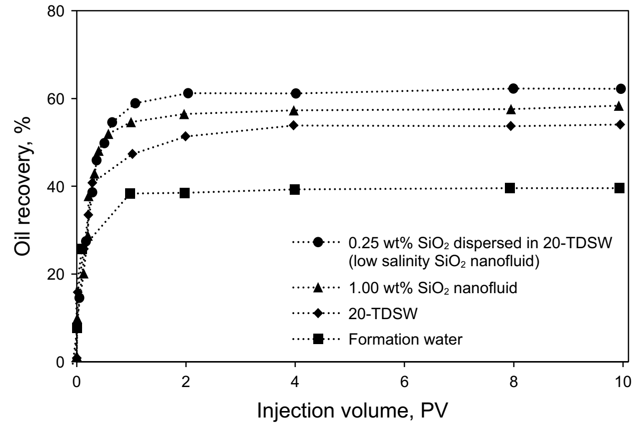

Fig. 14 Oil recovery during injection of formation water, 20-TDSW, 1.00 wt% SiO_2 nanofluid (prepared with deionized water) and 0.25 wt% of low-salinity SiO_2 nanofluid (prepared with 20-TDSW) into the treated (oil-wet) micromodels

Viscosity variation of different injection fluids and the differential pressure between the inlet and the outlet of the micromodel are shown in Fig. 17. Experimental viscosity data for different fluids were measured by an Ostwald viscometer under ambient conditions (25 °C and 1 atm). The characteristics of the viscometer were mentioned in our previous work (Dehaghani and Badizad 2016). In addition, differential pressures between the inlet and outlet of the micromodel at the start of injection and after 5 PV of injection were measured using an accurate barometer. According to these parameters, it can be concluded that by increasing the viscosity, the differential pressure would increase. Moreover, 1.00 wt% SiO_2 nanofluid had the highest viscosity (1.6 cP) of all. It is essential to note that the differential pressures after 5 PV for all injection fluids were less than what they were at the start of injection, that is, because of the establishment of continuous fluid flow. The latter occurred after 5 PV injection where a continuous flow of the displacing fluid with a lower viscosity in comparison with the displaced fluid will be established.

5 Conclusions

In this research, the synergic contribution of the low-salinity effect and SiO_2 nanoparticles were evaluated for EOR by conducting contact angle measurements and micromodel flooding. Major conclusions are drawn from this work:

1. The contact angle of the treated (oil-wet) glass surface after soaking in nanofluids with varying concentrations

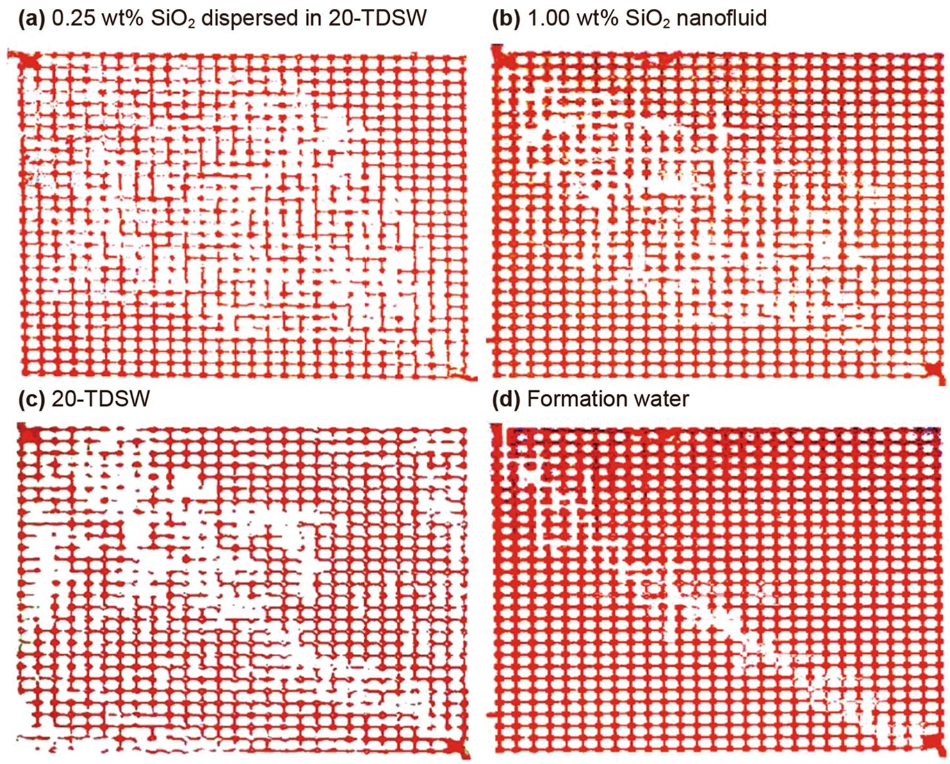

Fig. 15 Micromodel images of sweep efficiency during injection of 0.25 wt% of low-salinity SiO_2 nanofluid (prepared with 20-TDSW) (**a**), 1.00 wt% nanofluid (prepared with deionized water) (**b**), 20-TDSW (**c**), and formation water (**d**), into the treated (oil-wet) micromodels; all images were taken after 2 pore volume injection

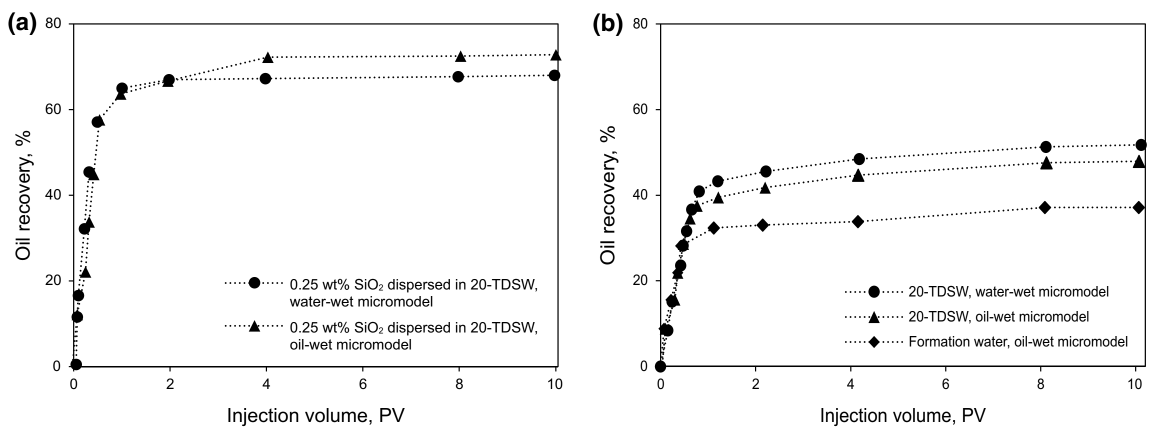

Fig. 16 Effect of the micromodel wettability on the oil recovery during injection of low-salinity nanofluids (0.25 wt%) (**a**) and 20-TDSW and formation water (**b**)

of dispersed SiO_2 particles demonstrates an abrupt change of wettability once the nanoparticle concentration increases above 0.75 wt%. To scrutinize the kinetic nature of wettability alteration, contact angle measurements were replicated over a longer period (for 6 days), but the deviation was insignificant.

2. Diluted samples of original seawater (SW) were ineffective in altering the contact angle at ambient temperature. However, contact angle measurements at 80 °C revealed the capability of diluted SW to change wetting toward a water-wet favorable state. This observation was ascribed to higher activities of dissolved ions at an elevated temperature.
3. The low-salinity effect was also active in the presence of dispersed SiO_2 nanoparticles. However, the nanofluid failed to change wettability in 100-fold dilution SW. In order to achieve a synergic contribution of both low-salinity effect and nanoparticles, an optimum concentration is needed. In the case of extraordinary dilution (here 100 times), the solution acts as does deionized water.
4. Micromodel flooding was performed to investigate displacement efficiency of SiO_2 nanofluids. The solution

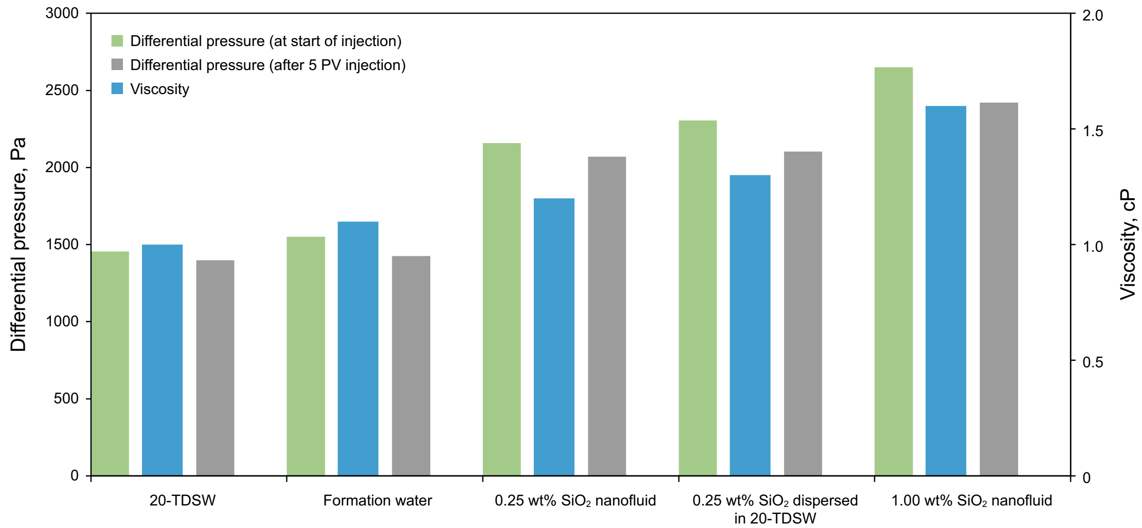

Fig. 17 Viscosity and differential pressure data for different injection fluids

containing 1.00 wt% nanoparticles displayed the longest breakthrough time in comparison with the diluted ones. Silica nanoparticles dispersed in the 20-fold diluted brine also affected the oil recovery very much. These experiments showed that the increase in breakthrough time is not only due to viscosity increment but also due to other mechanisms such as the salting in effect and the Brownian motion of silica nanoparticles.

5. Afterward, a 20 times diluted brine, 1.00 wt% silica nanofluid (prepared with deionized water) and a combined fluid of 0.25 wt% silica nanoparticles in a 20 times diluted brine were injected into oil-wet micromodels. The results indicated that the combination of silica nanoparticles and the 20 times diluted brine (low salinity) had a better influence in comparison with the nanofluid of higher silica concentrations and salinity of 0. The test also demonstrated that the combined fluid is more effective in oil-wet environments.
6. Comparison was made of silica nanoparticles in water-wet and oil-wet porous media, and it was concluded that in a water-wet medium the oil recovery was about 4% more than that in an oil-wet medium.
7. The effects of injecting the 20 times diluted brine and the formation water into oil-wet and water-wet micromodels were compared. The test proved that injecting formation water into an oil-wet porous medium led to lower oil recovery compared to the situation where the 20 times diluted brine was injected. The injection of the 20 times diluted brine into a water-wet porous medium also resulted in a higher oil recovery compared to the oil recovery obtained in an oil-wet porous medium. The latter indicates that the wettability of the porous medium is very effective for oil recovery; however, it is not the only factor controlling distributions of oil and other fluids in porous media.

Acknowledgement We acknowledge the support of INSF (Grant No. 96007551).

References

Agbalaka CC, Dandekar AY, Patil SL, Khataniar S, Hemsath JR. Coreflooding studies to evaluate the impact of salinity and wettability on oil recovery efficiency. Transp Porous Media. 2009;76(1):77. https://doi.org/10.1007/s11242-008-9235-7.

Aghaeifar Z, Strand S, Austad T, Puntervold T, Aksulu H, Navratil K, et al. Influence of formation water salinity/composition on the low-salinity enhanced oil recovery effect in high-temperature sandstone reservoirs. Energy Fuels. 2015;29(8):4747–54. https://doi.org/10.1021/acs.energyfuels.5b01621.

Al-Anssari S, Barifcani A, Wang S, Iglauer S. Wettability alteration of oil-wet carbonate by silica nanofluid. J Colloid Interface Sci. 2016;461:435–42. https://doi.org/10.1016/j.jcis.2015.09.051.

Al-Aulaqi T, Grattoni C, Fisher Q, Musina Z, Al-Harrasi M, Kapur N. Effect of temperature and salinity on wettability: microscale study. In: IOR 2011—16th European symposium on improved oil recovery; 2011a. https://doi.org/10.3997/2214-4609.201404774.

Al-Aulaqi T, Grattoni C, Fisher Q, Musina Z, Al-Hinai S. Effect of temperature, oil asphaltene content, and water salinity on wettability alteration. In: SPE/DGS Saudi Arabia section technical

symposium and exhibition; 2011b. https://doi.org/10.2118/149071-MS.
Al Harrasi A, Al-maamari RS, Masalmeh SK. Laboratory investigation of low salinity waterflooding for carbonate reservoirs. In: Abu Dhabi international petroleum conference and exhibition; 2012. https://doi.org/10.2118/161468-MS.
Alomair OA, Matar KM, Alsaeed YH. Nanofluids application for heavy oil recovery. In: SPE Asia Pacific oil and gas conference and exhibition; 2014. https://doi.org/10.2118/171539-MS.
Aurand KR, Dahle GS, Torsæter O. Comparison of oil recovery for six nanofluids in Berea sandstone cores. In: International symposium of the society of core analysts, September; 2014.
Barati-Harooni A, Najafi-Marghmaleki A, Tatar A, Mohammadi AH. Experimental and modeling studies on adsorption of a nonionic surfactant on sandstone minerals in enhanced oil recovery process with surfactant flooding. J Mol Liq. 2016;220:1022–32. https://doi.org/10.1016/j.molliq.2016.04.090.
Bera A, Belhaj H. Ionic liquids as alternatives of surfactants in enhanced oil recovery: a state-of-the-art review. J Mol Liq. 2016;224:177–88. https://doi.org/10.1016/j.molliq.2016.09.105.
Bondino I, Doorwar S, Ellouz R, Hamon G. Visual microscopic investigations about the role of pH, salinity and clay on oil adhesion and recovery. In: The international symposium of the society of core analysts, Napa Valley, California; 2013. SCA2013-021.
Brady PV, Krumhansl JL. A surface complexation model of oil–brine–sandstone interfaces at 100 °C: low salinity waterflooding. J Pet Sci Eng. 2012;81:171–6. https://doi.org/10.1016/j.petrol.2011.12.020.
Brady PV, Thyne G. Functional wettability in carbonate reservoirs. Energy Fuels. 2016;30(11):9217–25. https://doi.org/10.1021/acs.energyfuels.6b01895.
Brady PV, Morrow NR, Fogden A, Deniz V, Loahardjo N. Electrostatics and the low salinity effect in sandstone reservoirs. Energy Fuels. 2015;29(2):666–77. https://doi.org/10.1021/ef502474a.
Buckley J, Morrow N. Improved oil recovery by low salinity waterflooding: a mechanistic review. In: 11th international symposium on evaluation of wettability and its effect on oil recovery, Calgary; 2010.
Buckley JS. Evaluation of reservoir wettability and its effect on oil recovery: National Petroleum Technology Office, Tulsa, OK (US). 1999. https://doi.org/10.2172/8240.
Buckley SE, Leverett M. Mechanism of fluid displacement in sands. Trans AIME. 1942;146(01):107–16. https://doi.org/10.2118/942107-G.
Chengara A, Nikolov AD, Wasan DT, Trokhymchuk A, Henderson D. Spreading of nanofluids driven by the structural disjoining pressure gradient. J Colloid Interface Sci. 2004;280(1):192–201. https://doi.org/10.1016/j.jcis.2004.07.005.
Dehaghani AHS, Badizad MH. Experimental study of Iranian heavy crude oil viscosity reduction by diluting with heptane, methanol, toluene, gas condensate and naphtha. Petroleum. 2016;2(4):415–24. https://doi.org/10.1016/j.petlm.2016.08.012.
El-Diasty AI. The potential of nanoparticles to improve oil recovery in Bahariya Formation, Egypt: an experimental study. In: SPE Asia Pacific enhanced oil recovery conference; 2015. https://doi.org/10.2118/174599-MS.
Emadi A, Sohrabi M. Visual investigation of low salinity waterflooding. In: International symposium of the society of core analysts, Aberdeen, Scotland, UK; 2012.
Emadi A, Sohrabi M. Visual investigation of oil recovery by low salinity water injection: formation of water micro-dispersions and wettability alteration. In: SPE annual technical conference and exhibition; 2013: https://doi.org/10.2118/166435-MS.
Emadi S, Shadizadeh SR, Manshad AK, Rahimi AM, Mohammadi AH. Effect of nano silica particles on interfacial tension (IFT) and mobility control of natural surfactant (Cedr Extraction) solution in enhanced oil recovery process by nano-surfactant flooding. J Mol Liq. 2017;248:163–7. https://doi.org/10.1016/j.molliq.2017.10.031.
Fjelde I, Asen SM, Omekeh AV. Low salinity water flooding experiments and interpretation by simulations. In: SPE improved oil recovery symposium; 2012. https://doi.org/10.2118/154142-MS.
Fletcher A, Davis J. How EOR can be transformed by nanotechnology. In: SPE improved oil recovery symposium, 24–28 April, Tulsa, Oklahoma, USA; 2010. https://doi.org/10.2118/129531-MS.
Fredriksen SB, Rognmo AU, Fernø MA. Pore-scale mechanisms during low salinity waterflooding: water diffusion and osmosis for oil mobilization. In: SPE bergen one day seminar; 2016. https://doi.org/10.2118/180060-MS.
Gharibshahi R, Jafari A, Haghtalab A, Karambeigi MS. Application of CFD to evaluate the pore morphology effect on nanofluid flooding for enhanced oil recovery. RSC Adv. 2015;5(37):28938–49. https://doi.org/10.1039/C4RA15452E.
Green DW, Willhite GP. Enhanced oil recovery. Richardson: Doherty Memorial Fund of AIME, Society of Petroleum Engineers Richardson; 1998.
Haindade ZMW, Bihani AD, Javeri SM, Jere CB. Enhancing flow assurance using Co-Ni nanoparticles for dewaxing of production tubing. In: SPE international oilfield nanotechnology conference and exhibition; 2012. https://doi.org/10.2118/157119-MS.
Hashemi R, Nassar NN, Pereira Almao P. Enhanced heavy oil recovery by in situ prepared ultradispersed multimetallic nanoparticles: a study of hot fluid flooding for Athabasca bitumen recovery. Energy Fuels. 2013;27(4):2194–201. https://doi.org/10.1021/ef3020537.
Hendraningrat L, Torsæter O. Understanding fluid-fluid and fluid-rock interactions in the presence of hydrophilic nanoparticles at various conditions. In: SPE Asia Pacific oil & gas conference and exhibition; 2014a. https://doi.org/10.2118/171407-MS.
Hendraningrat L, Torsaeter O. Unlocking the potential of metal oxides nanoparticles to enhance the oil recovery. In: Offshore technology conference-Asia; 2014b. https://doi.org/10.4043/24696-MS.
Hendraningrat L, Li S, Torsæter O. A coreflood investigation of nanofluid enhanced oil recovery. J Pet Sci Eng. 2013;111:128–38. https://doi.org/10.1016/j.petrol.2013.07.003.
Hendraningrat L, Li S, Torsaeter O. Enhancing oil recovery of low-permeability Berea sandstone through optimised nanofluids concentration. In: SPE enhanced oil recovery conference; 2013b. https://doi.org/10.2118/165283-MS.
Hendraningrat L, Li S, Torsater O. Effect of some parameters influencing enhanced oil recovery process using silica nanoparticles: an experimental investigation. In: SPE reservoir characterization and simulation conference and exhibition; 2013c. https://doi.org/10.2118/165955-MS.
Heydarian A, Kharrat R, Hashemi A. The impact of sparkling mechanism on improving oil recovery in nano-particle injection through pseudo-3-dimensional micromodels. J Am Sci. 2012;8(11):379-84.
Hosseinzade Khanamiri H, Baltzersen Enge I, Nourani M, Stensen JÅ, Torsæter O, Hadia N. EOR by low salinity water and surfactant at low concentration: impact of injection and in situ brine composition. Energy Fuels. 2016;30(4):2705–13. https://doi.org/10.1021/acs.energyfuels.5b02899.
Idogun AK, Iyagba ET, Ukwotije-Ikwut RP, Aseminaso A. A review study of oil displacement mechanisms and challenges of nanoparticle enhanced oil recovery. In: SPE Nigeria annual international conference and exhibition; 2016. https://doi.org/10.2118/184352-MS.

Jackson MD, Al-Mahrouqi D, Vinogradov J. Zeta potential in oil-water-carbonate systems and its impact on oil recovery during controlled salinity water-flooding. Sci Rep. 2016;6:37363. https://doi.org/10.1038/srep37363.

Jalili Z, Tabrizy VA. Mechanistic study of the wettability modification in carbonate and sandstone reservoirs during water/low salinity water flooding. Energy Environ Res. 2014;4(3):78. https://doi.org/10.5539/eer.v4n3p78.

Kafili Kasmaei A, Rao DN. Is Wettability alteration the main cause for enhanced recovery in low-salinity waterflooding? SPE Reserv Eval Eng. 2015;18(02):228–35. https://doi.org/10.2118/169120-PA.

Karimi A, Fakhroueian Z, Bahramian A, Khiabani NP, Darabad JB, Azin R, et al. Wettability alteration in carbonates using zirconium oxide nanofluids: EOR implications. Energy Fuels. 2012;26(2):1028–36. https://doi.org/10.1021/ef201475u.

Kazempour M, Alvarado V, Manrique EJ, Izadi M. Impact of alkaline-surfactant-polymer flooding model on upscaled recovery predictions: medium and heavy oils. In: SPE heavy and extra heavy oil conference, Latin America; 2014. https://doi.org/10.2118/171055-MS.

Kazemzadeh Y, Eshraghi SE, Kazemi K, Sourani S, Mehrabi M, Ahmadi Y. Behavior of asphaltene adsorption onto the metal oxide nanoparticle surface and its effect on heavy oil recovery. Ind Eng Chem Res. 2015;54(1):233–9. https://doi.org/10.1021/ie503797g.

Lager A, Webb KJ, Black C, Singleton M, Sorbie KS. Low salinity oil recovery—an experimental investigation1. Petrophysics. 2008;49(01):28–35.

Li R, Jiang P, Gao C, Huang F, Xu R, Chen X. Experimental investigation of silica-based nanofluid enhanced oil recovery: the effect of wettability alteration. Energy Fuels. 2016;31(1):188–97. https://doi.org/10.1021/acs.energyfuels.6b02001.

Li S, Torsæter O. An experimental investigation of EOR mechanisms for nanoparticles fluid in glass micromodel. Paper SCA2014-022 was prepared for presentation at the International Symposium of the Society of Core Analysts held in Avignon, France; 2014.

Li S, Genys M, Wang K, Torsæter O. Experimental study of wettability alteration during nanofluid enhanced oil recovery process and its effect on oil recovery. In: SPE reservoir characterization and simulation conference and exhibition; 2015. https://doi.org/10.2118/175610-MS.

Li S, Hendraningrat L, Torsaeter O. Improved oil recovery by hydrophilic silica nanoparticles suspension: 2 phase flow experimental studies. In: International petroleum technology conference; 2013.

Ligthelm DJ, Gronsveld J, Hofman J, Brussee N, Marcelis F, van der Linde H. Novel waterflooding strategy by manipulation of injection brine composition. In: EUROPEC/EAGE conference and exhibition; 2009. https://doi.org/10.2118/119835-MS.

Maaref S, Ayatollahi S, Rezaei N, Masihi M. The effect of dispersed phase salinity on water-in-oil emulsion flow performance: a micromodel study. Ind Eng Chem Res. 2017;56(15):4549–61. https://doi.org/10.1021/acs.iecr.7b00432.

Maghzi A, Mohammadi S, Ghazanfari MH, Kharrat R, Masihi M. Monitoring wettability alteration by silica nanoparticles during water flooding to heavy oils in five-spot systems: a pore-level investigation. Exp Thermal Fluid Sci. 2012;40:168–76. https://doi.org/10.1016/j.expthermflusci.2012.03.004.

Mahani H, Keya AL, Berg S, Bartels W-B, Nasralla R, Rossen WR. Insights into the mechanism of wettability alteration by low-salinity flooding (LSF) in carbonates. Energy Fuels. 2015;29(3):1352–67. https://doi.org/10.1021/ef5023847.

Mahani H, Keya AL, Berg S, Nasralla R. Electrokinetics of carbonate/brine interface in low-salinity waterflooding: effect of brine salinity, composition, rock type, and pH on ζ-potential and a surface-complexation model. SPE J. 2017;22(01):53–68. https://doi.org/10.2118/181745-PA.

Mcelfresh PM, Holcomb DL, Ector D. Application of nanofluid technology to improve recovery in oil and gas wells. In: SPE international oilfield nanotechnology conference and exhibition; 2012. https://doi.org/10.2118/154827-MS.

McGuire P, Chatham J, Paskvan F, Sommer D, Carini F. Low salinity oil recovery: an exciting new EOR opportunity for Alaska's North Slope. In: SPE western regional meeting; 2005. https://doi.org/10.2118/93903-MS.

Mohammadi S, Maghzi A, Ghazanfari M, Masihi M, Kharrat R. On the effect of silica nanoparticles on wettability alteration during water flooding to heavy oils: a micromodel study. In: 74th EAGE conference and exhibition incorporating EUROPEC 2012; 2012. https://doi.org/10.3997/2214-4609.20148647.

Mohebbifar M, Ghazanfari MH, Vossoughi M. Experimental investigation of nano-biomaterial applications for heavy oil recovery in Shaly porous models: a pore-level study. J Energy Res Technol. 2015;137(1):014501. https://doi.org/10.1115/1.4028270.

Morrow N, Buckley J. Improved oil recovery by low-salinity waterflooding. J Pet Technol. 2011;63(05):106–12. https://doi.org/10.2118/129421-JPT.

Morrow NR, Tang G, Valat M, Xie X. Prospects of improved oil recovery related to wettability and brine composition. J Pet Sci Eng. 1998;20(3):267–76. https://doi.org/10.1016/s0920-4105(98)00030-8.

Nasralla RA, Nasr-El-Din HA. Double-layer expansion: is it a primary mechanism of improved oil recovery by low-salinity waterflooding? SPE Reservoir Eval Eng. 2014;17(01):49–59. https://doi.org/10.2118/154334-PA.

Nassar NN, Hassan A, Pereira-Almao P. Thermogravimetric studies on catalytic effect of metal oxide nanoparticles on asphaltene pyrolysis under inert conditions. J Therm Anal Calorim. 2012;110(3):1327–32. https://doi.org/10.1007/s10973-011-2045-0.

Parvazdavani M, Masihi M, Ghazanfari MH, Sherafati M, Mashayekhi L. Investigation of the effect of water based nano-particles addition on hysteresis of oil-water relative permeability curves. In: SPE international oilfield nanotechnology conference and exhibition; 2012. https://doi.org/10.2118/157005-MS.

Ragab AMS, Hannora AE. An experimental investigation of silica nano particles for enhanced oil recovery applications. In: SPE North Africa technical conference and exhibition; 2015. https://doi.org/10.2118/175829-MS.

Rezaei A, Abdi-Khangah M, Mohebbi A, Tatar A, Mohammadi AH. Using surface modified clay nanoparticles to improve rheological behavior of hydrolyzed polyacrylamide (HPAM) solution for enhanced oil recovery with polymer flooding. J Mol Liq. 2016;222:1148–56. https://doi.org/10.1016/j.molliq.2016.08.004.

RezaeiDoust A, Puntervold T, Strand S, Austad T. Smart water as wettability modifier in carbonate and sandstone: a discussion of similarities/differences in the chemical mechanisms. Energy Fuels. 2009;23(9):4479–85. https://doi.org/10.1021/ef900185q.

Rezvani H, Khalilnezhad A, Ganji P, Kazemzadeh Y. How ZrO_2 nanoparticles improve the oil recovery by affecting the interfacial phenomena in the reservoir conditions? J Mol Liq. 2017. https://doi.org/10.1016/j.molliq.2017.12.138.

Rivet S, Lake LW, Pope GA. A coreflood investigation of low-salinity enhanced oil recovery. In: SPE annual technical conference and exhibition; 2010. https://doi.org/10.2118/134297-MS.

Salem Ragab AM, Hannora AE. A comparative investigation of nano particle effects for improved oil recovery—experimental work. In: SPE Kuwait oil and gas show and conference; 2015. https://doi.org/10.2118/175395-MS.

Shabib-Asl A, Mohammed MAA, Kermanioryani M, Valentim PPJ. Effects of low salinity water ion composition on wettability alteration in sandstone reservoir rock: a laboratory investigation. J Nat Sci Res. 2014;4(13):34–41.

Shaddel S, Tabatabae-Nejad SA, Fathi SJ. Low-salinity water flooding: evaluating the effect of salinity on oil and water relative permeability, wettability, and oil recovery. Spec Top Rev Porous Media Int J. 2014. https://doi.org/10.1615/specialtopicsrevporousmedia.v5.i2.40.

Sheng J. Modern chemical enhanced oil recovery: theory and practice. Houston: Gulf Professional Publishing; 2010.

Sheng J. Critical review of low-salinity waterflooding. J Pet Sci Eng. 2014;120:216–24. https://doi.org/10.1016/j.petrol.2014.05.026.

Song W, Kovscek AR. Functionalization of micromodels with kaolinite for investigation of low salinity oil-recovery processes. Lab Chip. 2015;15(16):3314–25. https://doi.org/10.1039/C5LC00544B.

Sun X, Zhang Y, Chen G, Gai Z. Application of nanoparticles in enhanced oil recovery: a critical review of recent progress. Energies. 2017;10(3):345. https://doi.org/10.3390/en10030345.

Tang G, Morrow NR. Salinity, temperature, oil composition, and oil recovery by waterflooding. SPE Reserv Eng. 1997;12(04):269–76. https://doi.org/10.2118/36680-PA.

Tang G-Q, Morrow NR. Influence of brine composition and fines migration on crude oil/brine/rock interactions and oil recovery. J Pet Sci Eng. 1999a;24(2–4):99–111. https://doi.org/10.1016/S0920-4105(99)00034-0.

Tang G-Q, Morrow NR. Influence of brine composition and fines migration on crude oil/brine/rock interactions and oil recovery. J Pet Sci Eng. 1999b;24(2):99–111. https://doi.org/10.1016/S0920-4105(99)00034-0.

Tang G, Morrow N. Oil recovery by water flooding and imbibition–invading brine cation valency and salinity. Paper SCA-9911. 1999c.

Tang G, Morrow NR. Injection of dilute brine and crude oil/brine/rock interactions. In: Environmental Mechanics: Water, Mass and Energy Transfer in the Biosphere: The Philip Volume. 2002. p. 171–9. https://doi.org/10.1029/129gm16.

Tarboush BJA, Husein MM. Adsorption of asphaltenes from heavy oil onto in situ prepared NiO nanoparticles. J Colloid Interface Sci. 2012;378(1):64–9. https://doi.org/10.1016/j.jcis.2012.04.016.

Tarek M, El-Banbi AH. Comprehensive investigation of effects of nano-fluid mixtures to enhance oil recovery. In: SPE North Africa technical conference and exhibition; 2015. https://doi.org/10.2118/175835-MS.

Torsater O, Engeset B, Hendraningrat L, Suwarno S. Improved oil recovery by nanofluids flooding: an experimental study. In: SPE Kuwait international petroleum conference and exhibition; 2012. https://doi.org/10.2118/163335-MS.

Wang H, Liao X, Zhao X. The influence of CO_2 solubility in reservoir water on CO_2 flooding and storage of CO_2 injection into a water flooded low permeability reservoir. Energy Sources Part A Recov Util Environ Eff. 2014;36(8):815–21. https://doi.org/10.1080/15567036.2012.741654.

Wasan D, Nikolov A, Kondiparty K. The wetting and spreading of nanofluids on solids: role of the structural disjoining pressure. Curr Opin Colloid Interface Sci. 2011;16(4):344–9. https://doi.org/10.1016/j.cocis.2011.02.001.

Wei B, Lu L, Li Q, Li H, Ning X. Mechanistic study of oil/brine/solid interfacial behaviors during low-salinity water flooding using visual and quantitative methods. Energy Fuels. 2017. https://doi.org/10.1021/acs.energyfuels.7b00825.

Wu Z, Liu H, Pang Z, Wu Y, Wang X, Gao M. Visualized study on blocking characteristics and EOR mechanisms of high-temperature gel during steam injection process. In: International petroleum technology conference, 14–16 November, Bangkok, Thailand; 2016a. https://doi.org/10.2523/IPTC-18622-MS. https://doi.org/10.2523/IPTC-18622-MS.

Wu Z, Liu H, Pang Z, Wu Y, Wang X, Liu D, et al. A visual investigation of enhanced heavy oil recovery by foam flooding after hot water injection. J Pet Sci Eng. 2016;147:361–70. https://doi.org/10.1016/j.petrol.2016.08.023.

Xie Q, Chen Y, Sari A, Pu W, Saeedi A, Liao X. A pH-resolved wettability alteration: implications for CO_2-assisted EOR in carbonate reservoirs. Energy Fuels. 2017;31(12):13593–9. https://doi.org/10.1021/acs.energyfuels.7b03071.

Xie Q, Saeedi A, Pooryousefy E, Liu Y. Extended DLVO-based estimates of surface force in low salinity water flooding. J Mol Liq. 2016;221:658–65. https://doi.org/10.1016/j.molliq.2016.06.004.

Yang J, Dong Z, Dong M, Yang Z, Lin M, Zhang J, et al. Wettability alteration during low-salinity waterflooding and the relevance of divalent ions in this process. Energy Fuels. 2015;30(1):72–9. https://doi.org/10.1021/acs.energyfuels.5b01847.

Zamani A, Maini B, Pereira-Almao P. Flow of nanodispersed catalyst particles through porous media: effect of permeability and temperature. Can J Chem Eng. 2012;90(2):304–14. https://doi.org/10.1002/cjce.20629.